

Size and structural dependence of the magnetic properties of rhodium clusters

P. Villaseñor-González and J. Dorantes-Dávila

Instituto de Física "Manuel Sandoval Vallarta," Universidad Autónoma de San Luis Potosí, 78000 San Luis Potosí, Mexico

H. Dreyssé

Institut de Physique et Chimie des Matériaux de Strasbourg, Université Louis Pasteur, 23 rue du Loess, F-67037 Strasbourg, France

G. M. Pastor

Laboratoire de Physique Quantique, 118 route de Narbonne, Université Paul Sabatier, F-31062 Toulouse, France

(Received 21 August 1996; revised manuscript received 11 December 1996)

The size and structural dependence of the magnetic properties of Rh_N clusters ($9 \leq N \leq 55$) are studied by using a d -electron tight-binding Hamiltonian including Coulomb interactions in the unrestricted Hartree-Fock approximation. Three main different types of cluster geometries are considered (viz., fcc, bcc, and icosahedral). In each case the equilibrium bond length R is optimized by maximizing the cohesive energy $E_{\text{coh}}(N)$. The geometries yielding the largest $E_{\text{coh}}(N)$ alternate as a function of N . These structural changes, together with the variation of R , play a crucial role in the determination of the average magnetic moment $\bar{\mu}_N$ of Rh_N . The calculated size dependence of $\bar{\mu}_N$ corresponding to the most stable geometries presents oscillations which are in good qualitative agreement with experiment. The magnetic properties of Rh_N clusters show a remarkable structural dependence which is characteristic of weak (unsaturated) itinerant ferromagnetism. The relation between the observed $\bar{\mu}_N$ and the cluster geometry is analyzed. The role of nonuniform geometry relaxation, sp electrons, and sp - d hybridization effects are quantified for representative examples. Perspectives of extensions of this study are also discussed. [S0163-1829(97)08617-7]

I. INTRODUCTION

It is well known that atoms having an open shell, and transition metal (TM) atoms in particular, are all magnetic. This is a consequence of the Coulomb repulsion among the electrons which tends to maximize the total spin S , as stated by Hund's rules.¹ In the corresponding solids, however, the kinetic energy associated with d -electron delocalization and band formation plays a major role. It favors a nonmagnetic ground state and in the end the elements being magnetic in the macroscopic limit are rather few.² In fact, none of the $4d$ and $5d$ TM solids are magnetic in equilibrium conditions. These and other qualitative differences between atomic and solid-state magnetism have motivated in past years numerous studies of the magnetic properties of finite-size clusters, which behavior should interpolate somehow between these two limits.³⁻²⁰ In this context, one of the questions which attracted considerable attention is the possibility of the onset of magnetism as the dimensions of the system are reduced, i.e., in clusters of elements which are nonmagnetic in the bulk.¹¹⁻²⁰

Recently, Cox *et al.* have observed experimentally that Rh_N clusters have a permanent magnetic moment for $N \leq 60-90$, whereas Ru_N and Pd_N appear to be nonmagnetic at least for $N > 13$.¹⁴ The case of Rh is the first one where magnetism is observed in clusters of a nonmagnetic solid. The average magnetic moment per atom $\bar{\mu}_N$ of Rh_N derived from experiment shows in addition a remarkable size dependence. Within a reduced size range ($N \leq 60-90$), $\bar{\mu}_N$ decreases from rather large values for the smallest clusters [e.g., $\mu_9 = (0.8 \pm 0.2)\mu_B$] to very small (if not vanishing) values [e.g., $\bar{\mu}_{30} = (0.13 \pm 0.14)\mu_B$ and $\mu_{60} = (0.05$

$\pm 0.1)\mu_B$]. Moreover, $\bar{\mu}_N$ oscillates as a function of N , showing maxima and minima at certain cluster sizes. For example, $\bar{\mu}_N$ is particularly large for $N = 15-16$ and 19 and drops for $N = 13-14$, $17-18$, and 20 .¹⁴ This behavior is different from what is observed in ferromagnetic TM's such as Fe_N , Co_N , and Ni_N , where the variations of $\bar{\mu}_N$ are relatively less important and extend over a much wider range of cluster sizes.^{7,8} It would be therefore of considerable interest to understand the electronic origin of the size dependence of the magnetic moments of Rh_N clusters and, if possible to correlate it with the changes in the local environment of the atoms which occur as a function of N , for example, the changes in the symmetry and interatomic bond lengths.

The large majority of the available theoretical results on Rh_N clusters are mainly based on the local spin-density approximation (LSDA).¹⁵⁻¹⁹ In these studies the electronic and magnetic properties of Rh_N have been determined for a few cluster sizes assuming (except for the very small ones) highly symmetric cluster structures. Galicia,¹⁵ Reddy *et al.*,¹⁶ and Piveteau *et al.*²⁰ considered Rh_{13} and obtained that it is magnetic. Jinlong *et al.*^{17,18} studied several Rh_N clusters ($N = 2-8, 10, 12, 13$, and 19) and Li *et al.*¹⁹ calculated the magnetic properties of Rh_N for $N = 6, 9, 13, 19$, and 43 . In qualitative agreement with experiment one has found that small Rh_N clusters have a nonvanishing magnetization at $T = 0$.¹⁵⁻²⁰ However, the actual results for $\bar{\mu}_N$ are dispersed quantitatively. For instance, $\bar{\mu}_{13} = 1.00\mu_B$ after Ref. 15, $\bar{\mu}_{13} = 1.62\mu_B$ after Ref. 16, $\bar{\mu}_{13} = 1.15\mu_B$ after Ref. 17, $\bar{\mu}_{13} = 0.69\mu_B$ after Ref. 19, and $\bar{\mu}_{13} = 1.69\mu_B$ after Ref. 20. It has been pointed out^{18,19} that these differences might be due to the existence of different self-consistent solutions to the

Kohn-Sham equations. One may further notice that in the case of Rh clusters we are dealing with a system showing weak, nonsaturated, itinerant magnetism. In this case it is known^{9,21} that the magnetic behavior is very sensitive to the details of the local atomic environment and of the electronic density distribution which are somewhat different in these various studies.^{15–20} Besides these quantitative aspects, the values of N considered in the calculations available so far are rather few. This precludes to address the problem of the size dependence of $\bar{\mu}_N$ and in particular the possible origin of the oscillations observed experimentally. It is one of the purposes of this paper to investigate this problem by performing calculations for a larger number of cluster sizes and structures, particularly in the experimentally most interesting range $9 \leq N \leq 23$.

One of the main difficulties in the theoretical study of free clusters is the determination of the geometrical arrangement of the atoms, especially since direct experimental information is extremely difficult to obtain. This general problem is particularly delicate in the case of itinerant magnetism due to the strong sensitivity electronic structure and magnetic behavior to the lattice structure.^{9,21} Moreover, the localized character of the d -electron states and the complicated dependence of the magnetic moments and magnetic order on the cluster structure have made the application of first-principles geometry optimization procedures impracticable except for very small clusters. For not too small clusters, the only alternative left is to consider several cluster structures based on different local arrangement of the atoms (for example, fcc-like, bcc-like, or icosahedral-like) and to perform then a restricted optimization or relaxation preserving the proposed cluster symmetry. This is the procedure followed in this paper. However, the limitations of this approach should be kept in mind. Even if in some limiting cases the structure is known (e.g., the fcc structure of bulk Rh) the possible *a priori* choices for the atomic arrangements are almost unlimited, and many cases are known where “reasonable” structures are outruled by distorted or “unexpected” geometrical arrangements. As stated above, we are not able to attempt to solve this problem here. A rigorous, though model limited study of this matter may be found in Ref. 21. Nevertheless, considering several different structures allows us to quantify the structural dependence of the magnetic properties and to get a rough idea of the magnetic and energetic surfaces in configuration space. Moreover, the result can be compared to experiment from two different points of views: first, by using the values of $\bar{\mu}_N$ corresponding to the structure yielding the largest calculated cohesive energy and, second, by analyzing the size dependence of $\bar{\mu}_N$ corresponding to different symmetries. In this way the experimental information on the size dependence of $\bar{\mu}_N$ can be used to discriminate between different geometrical arrangements.

The remainder of the paper is organized as follows. The theoretical framework used for the calculations is summarized in Sec. II. In Sec. III the results for Rh clusters are presented and discussed in particular by comparison with experiment and other calculations. We conclude in Sec. IV by discussing some of the limitations of the present approach together with relevant extensions.

II. THEORETICAL MODEL

The tight-binding method has been shown to provide an appropriate scheme for studying the environment dependence of TM magnetism in low-dimensional arrangements^{9,22} and in particular the size and structural dependence of the magnetic properties of TM clusters.^{9,11,13} In the following we consider a d -band model Hamiltonian H which includes intra-atomic Coulomb interactions self-consistently within the unrestricted Hartree-Fock approximation.⁹ For simplicity only the $4d$ electrons are considered explicitly in the calculations, since they are expected to dominate the magnetic behavior, as it is the case for $3d$ electrons in the Fe series (see, for instance, Ref. 23). Some of the possible consequences of this approximation will be discussed in Sec. IV. In the usual notation,

$$H = \sum_{i\alpha\sigma} \varepsilon_{i\alpha\sigma} \hat{n}_{i\alpha\sigma} + \sum_{\substack{\alpha,\beta,\sigma \\ i \neq j}} t_{ij}^{\alpha\beta} \hat{c}_{i\alpha\sigma}^\dagger \hat{c}_{j\beta\sigma}, \quad (2.1)$$

where $t_{ij}^{\alpha\beta}$ refers to the hopping integral between the d orbitals α and β ($\alpha, \beta \equiv xy, xz, yz, x^2 - y^2, 3z^2 - r^2$) at sites i and j and

$$\varepsilon_{i\alpha\sigma} = \varepsilon_\alpha^0 + \sum_{\beta\sigma'} U_{\alpha\beta}^{\sigma\sigma'} \Delta \nu_{i\beta\sigma'} \quad (2.2)$$

stands for the site-dependent d energy levels. In Eq. (2.2), ε_α^0 indicates the d energy level of the solid (paramagnetic solution) and the second term takes into account the shifts due to the redistribution of the spin-polarized electronic density which occurs in the cluster. $\Delta \nu_{i\beta\sigma} = \nu_{i\beta\sigma} - \nu_{i\beta\sigma}^0$, where $\nu_{i\beta\sigma} = \langle \hat{n}_{i\beta\sigma} \rangle$ is the average occupation of the spin orbital $i\beta\sigma$ and $\nu_{i\beta\sigma}^0$ is the corresponding average occupation in the solid. The number of d electrons at site i ,

$$\nu(i) = \sum_\alpha (\langle \hat{n}_{i\alpha\uparrow} \rangle + \langle \hat{n}_{i\alpha\downarrow} \rangle), \quad (2.3)$$

and the local magnetic moments

$$\mu(i) = \sum_\alpha (\langle \hat{n}_{i\alpha\uparrow} \rangle - \langle \hat{n}_{i\alpha\downarrow} \rangle) \quad (2.4)$$

are determined self-consistently by requiring

$$\langle \hat{n}_{i\alpha\sigma} \rangle = \int_{-\infty}^{\varepsilon_F} \rho_{i\alpha\sigma}(\varepsilon) d\varepsilon. \quad (2.5)$$

The local density of states (LDOS) $\rho_{i\alpha\sigma}(\varepsilon) = (-1/\pi) \text{Im}\{G_{i\alpha\sigma, i\alpha\sigma}(\varepsilon)\}$ is obtained from the local Green's functions $G_{i\alpha\sigma, i\alpha\sigma}(\varepsilon)$ by using the recursion method.²⁴ The number of levels M of the continued fraction expansion of $G_{i\alpha\sigma, i\alpha\sigma}$ is such that $\rho_{i\alpha\sigma}(\varepsilon)$ corresponds to the exact solution of the single-particle problem. The size-dependent Fermi energy ε_F is obtained from the global charge neutrality condition $\sum_i \nu(i) = Nn_d$, where n_d refers to the number of d electrons per atom. Notice that spin-polarized charge transfers between atoms and orbitals having different local environments will generally occur.

In order to determine the optimum interatomic bond lengths and the relative stability between different structures, we consider the cohesive energy per atom which is given by

$$E_{\text{coh}}(N) = E_b(1) - E_b(N) - E_R. \quad (2.6)$$

The electronic d -band energy per atom,

$$E_b(N) = \frac{1}{N} \sum_{i=1}^N \sum_{\alpha\sigma} \int_{-\infty}^{e_F} \varepsilon \rho_{i\alpha\sigma}(\varepsilon) d\varepsilon - E_{\text{DC}}, \quad (2.7)$$

represents the sum of the single-particle eigenvalues minus the double counting term $E_{\text{DC}} = (1/2N) \sum_{i\alpha\sigma} (\varepsilon_{i\alpha\sigma} - \varepsilon_{\alpha}^0) \langle \hat{n}_{i\alpha\sigma} \rangle$.⁹ E_b includes the contributions resulting from the distance dependence of the hopping integrals $t_{ij}^{\alpha\beta}$ and from the changes in the local magnetic moments $\mu(i)$ in particular. The repulsive interactions E_R are approximated by a Born-Mayer pair potential

$$E_R = \frac{A}{2} \sum_{i \neq j} e^{-\kappa(R_{ij} - R_0)/R_0}, \quad (2.8)$$

where $R_{ij} = |\vec{R}_j - \vec{R}_i|$ refers to the interatomic distance and R_0 to the nearest-neighbor (NN) distance in the solid.^{9,31} The parameters A and κ are obtained from the bulk equilibrium condition and compressibility modulus. Notice, however, that a much better transferability of the repulsive interactions is obtained when nonorthogonality effects are treated explicitly.^{32,33}

III. RESULTS

In this section we present and discuss our results for magnetic properties of Rh_N clusters ($N \leq 55$) as obtained using the model described in the previous section. The parameters involved in the calculations are determined as follows. The hopping integrals $t_{ij}^{\alpha\beta}$ are given by the canonical expression in terms of the two-center integrals $t_{ij}(\sigma, \pi, \delta) = (-6, 4, -1)(W_b/W_0)(R_0/R_{ij})^5$ where $W_b = 7.4$ eV is the bulk d -band width and W_0 is a dimensionless constant.²⁶ The direct Coulomb integral U and the exchange integral J , being intra-atomic parameters, are taken to be independent of interatomic distances. The value of $U = 7.8$ eV is estimated from the difference between the ionization potential and electron affinity of the Rh atom. Note that the magnetic properties are not affected by reasonable variations of U , since local charge neutrality is approximately satisfied.⁹ The exchange integral $J = 0.48$ is obtained from LSDA Stoner theory^{27,28} by taking into account a reduction of 20% due to correlation effects beyond the LSDA.²⁹ Applying this procedure to Fe one obtains $J_{\text{Fe}} = 0.71$ eV, which is very close to the value $J_{\text{Fe}} = 0.69$ eV yielding the proper Fe-bulk magnetization.⁹ The sensitivity of the magnetic moments to J shall be discussed later on. The number of d electrons $n_d = 8.0$ corresponds approximately to Rh bulk³⁰ as well as to Rh clusters.^{17,18} Finally, the Born-Mayer parameters $A = 0.136$ eV and $\kappa = 14.4$ are obtained by fitting the equilibrium condition at $R = R_0$ and the compressibility modulus of the solid.²

In Table I results are given for the size and structural dependence of various electronic and magnetic properties of Rh_N clusters, namely, the cohesive energy per atom

TABLE I. Size and structural dependence of the electronic and magnetic properties of Rh_N clusters. Results are given for the cohesive energy per atom, E_{coh} (in eV), the equilibrium bond length R/R_0 ($R_0 =$ bulk NN distance), the average magnetic moment per atom $\bar{\mu}_N$ (in units of μ_B), and the local magnetic moments $\mu(i)$ at the different symmetry atoms i as labeled in Fig. 1. We consider bcc-like (bcc), fcc-like (fcc), and icosahedral-like (ico) structures as well as the twisted double square (tw) for $N=9$. For the fcc-like cluster with $N=11$, a and b correspond to different arrangements of the atoms in the outer open shell. For $N=20$, $\mu(i)$ at shell i refers to the average within the i th NN shell of atom 1 (see Fig. 1).

Cluster	E_{coh}	R/R_0	$\bar{\mu}_N$	$\mu(1)$	$\mu(2)$	$\mu(3)$	$\mu(4)$	$\mu(5)$
tw ₉	2.38	0.95	0.66	-0.13	0.71	0.79		
fcc ₉	2.34	0.93	0.22	-0.03	0.24			
bcc ₉	2.29	0.88	1.34	0.34	1.44			
ico ₁₁	2.43	0.98	0.73	-0.13	0.83			
fcc ₁₁ ^a	2.43	0.95	0.18	-0.04	0.18	0.16	0.18	
fcc ₁₁ ^b	2.41	0.95	0.18	0.07	0.15	0.22	0.14	0.15
bcc ₁₁	2.36	0.91	0.73	-0.10	0.80	0.57		
bcc ₁₃	2.41	0.93	0.62	0.16	0.56	0.83		
ico ₁₃	2.38	0.93	0.92	0.09	0.97			
fcc ₁₃	2.38	0.96	0.77	0.26	0.81			
fcc ₁₅	2.44	0.96	0.80	0.78	0.99	0.92	-0.27	
bcc ₁₅	2.36	0.95	1.33	0.05	1.24	1.58		
fcc ₁₇	2.46	0.98	0.71	1.21	0.84	0.97	0.03	
fcc ₁₉	2.52	0.97	0.95	1.16	1.07	0.64		
ico ₁₉	2.48	0.89	0.11	0.20	0.14	0.00	-0.07	
bcc ₁₉	2.48	0.93	0.21	0.01	0.19	0.05	0.33	0.49
fcc ₂₀	2.52	0.97	0.70	0.95	0.82	0.50	-0.30	
bcc ₂₃	2.52	0.93	0.35	0.23	0.25	0.06	0.25	0.62
fcc ₂₇	2.53	0.97	0.67	0.42	0.49	0.59	0.98	
bcc ₂₇	2.50	0.94	0.59	0.26	0.41	0.06	0.98	
fcc ₄₃	2.63	0.98	0.28	0.51	0.26	0.02	0.39	
bcc ₅₁	2.60	0.95	0.43	0.05	0.10	0.14	0.43	0.61
ico ₅₅	2.75	0.96	0.00	0.00	0.00	0.00	0.00	
fcc ₅₅	2.68	0.98	0.44	-0.31	0.19	0.15	0.57	0.60
bulk	3.07	1.00	0.00					

$E_{\text{coh}}(N)$, the equilibrium NN bond length R/R_0 , the average magnetic moment per atom $\bar{\mu}_N$, and the local magnetic moments $\mu(i)$ at the different symmetry atoms i as labeled in Fig. 1. Three main different types of clusters structures are considered in the calculations: fcc-like, icosahedral-like, and bcc-like. For Rh_9 we shall also consider the twisted double-square pyramid. These structures are illustrated in Fig. 1 for some representative sizes. For each structure the NN bond length R is optimized by maximizing the cohesive energy, Eq. (2.6), with respect to the uniform relaxation. As in the case of $3d$ TM clusters [e.g., Fe_N and Ni_N (Ref. 9)] important bond-length contractions are obtained ($R/R_0 = 0.91 - 0.98$) which are quantitatively comparable to previous results on Rh_N .¹⁶⁻¹⁹ The bond-length relaxation plays an important

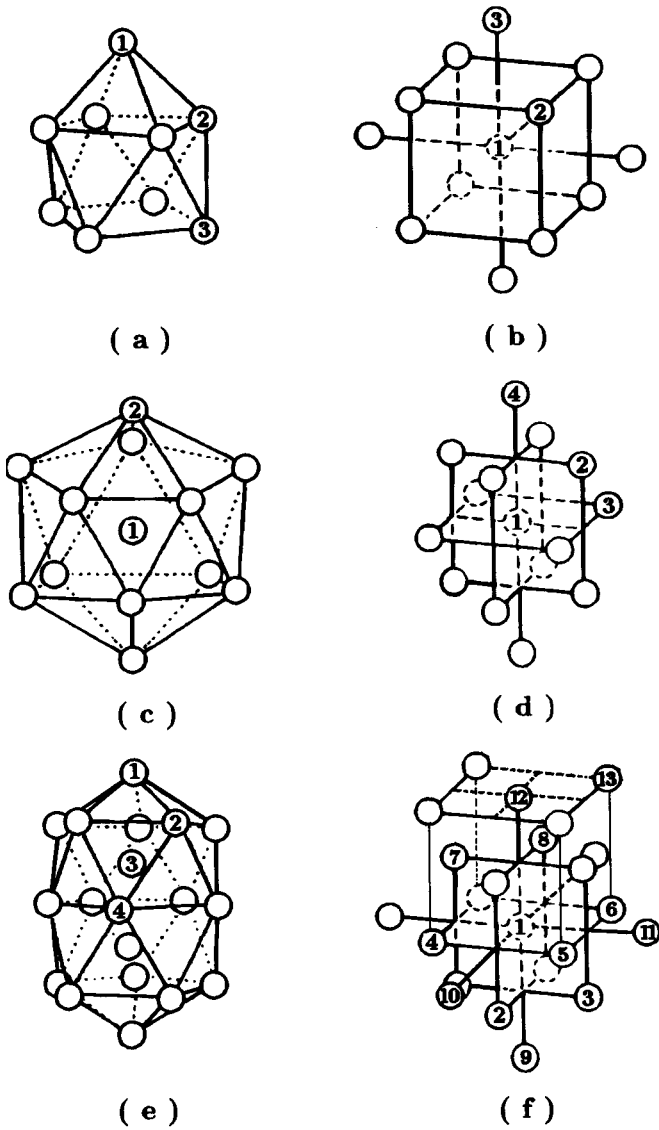


FIG. 1. Illustration of representative cluster structures considered in the calculations: (a) twisted double square for $N=9$, (b) bcc-like for $N=13$, (c) icosahedron for $N=13$, (d) fcc-like for $N=15$, (e) double icosahedron for $N=19$, and (f) fcc-like for $N=20$. The numbers indicate the different nonequivalent sites i in the cluster.

role on the relative stability of different structures and on the magnetic behavior of the cluster. Indeed, using the bulk NN distance ($R=R_0$) results in large overestimation of the local magnetic moments. For example, for an fcc-like 13-atom cluster we obtain $\bar{\mu}_{13}(R=R_0)=1.56\mu_B$ while the equilibrium value is $\bar{\mu}_{13}(R/R_0=0.97)=0.73\mu_B$. One may already conclude that the magnetic properties of Rh_N clusters are very sensitive to the local atomic environment. An interesting size and structural dependence can be expected, as it will be discussed below.

In Fig. 2 results are given for the size dependence of the average magnetic moment $\bar{\mu}_N$ of Rh_N corresponding to the most stable of the considered structures. The experimental results for $\bar{\mu}_N$ of Ref. 14 are also given for the sake of comparison. The calculated $\bar{\mu}_N$ oscillates as a function of

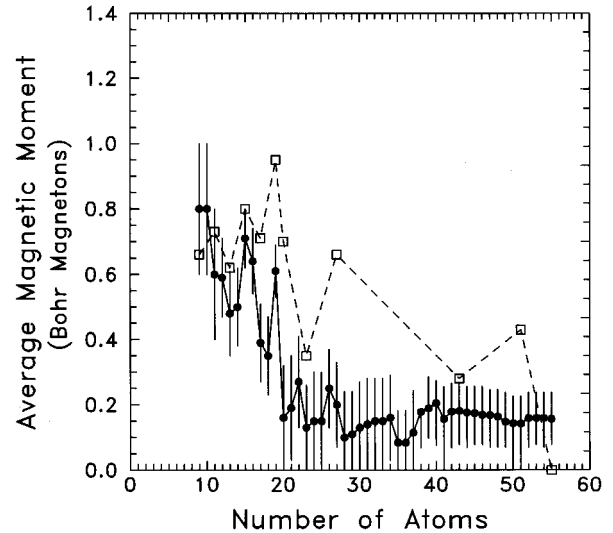


FIG. 2. Average magnetic moment $\bar{\mu}_N$ of Rh_N clusters as a function of N . The open squares refer to calculations for the most stable uniformly relaxed structure. The experimental results from Ref. 14 are indicated by dots and error bars. The dashed line is just a guide to the eye.

N and tends to decrease for increasing N . For $N=9$ the twisted double-square pyramid (tw) yields the largest $E_{\text{coh}}(N)$. The corresponding average magnetic moment is in good agreement with experiment [$\bar{\mu}_9^{\text{expt}}=(0.8\pm 0.2)\mu_B$ and $\bar{\mu}_9(\text{tw})=0.66\mu_B$]. For $N=11$ the icosahedral-like structure is more stable than the bcc- and fcc-like. However, the cohesive energy of one of the fcc-like clusters, $E_{\text{coh}}(\text{fcc}_{11}^q)$, is very close to $E_{\text{coh}}(\text{ico}_{11})$ and the approximations involved in our model do not allow us to discern safely between these two structures. However, the magnetic moments are much more structure sensitive in this case. While $\bar{\mu}_{11}(\text{ico})=0.73\mu_B$ is in good agreement with the experimental result [$\bar{\mu}_{11}^{\text{expt}}=(0.8\pm 0.2)\mu_B$], the result for the fcc structure differs significantly [$\bar{\mu}_{11}(\text{fcc})=0.18\mu_B$]. For $N=13$ the most stable geometrical configuration is the bcc-like structure which has a rather low symmetry and which was not considered in previous studies.^{15–20} The corresponding average magnetic moment, $\bar{\mu}_{13}(\text{bcc})=0.62\mu_B$, agrees with the experimental result $\bar{\mu}_{13}^{\text{expt}}=(0.48\pm 0.13)\mu_B$. For large values of N ($15\leq N\leq 43$) the fcc-like clusters are the most stable ones. However, for these larger clusters there are numerous possible configurations of the atoms in the outer shells and our geometry explorations are far from being extensive, even if the local environment is restricted to be fcc-, bcc-, or icosahedral-like. Notice that in this size range, the calculated $\bar{\mu}_N$ for fcc clusters are systematically larger than the experimental findings. Nevertheless, several trends concerning the size dependence of $\bar{\mu}_N$ are in qualitative agreement with experiment, in particular the local minima at $N=13, 17,$ and 20 and maxima at $N=15, 19,$ and 27 (see Fig. 3). For $N=55$, the icosahedral structure, which is nonmagnetic [$\bar{\mu}_{55}(\text{ico})=0\mu_B$] is more stable than the fcc structure [$\bar{\mu}_{55}(\text{fcc})=0.43\mu_B$].

It is interesting to attempt to relate the size dependence of $\bar{\mu}_N$ and, in particular, its oscillations with the size dependence of the cluster structure and equilibrium bond length.

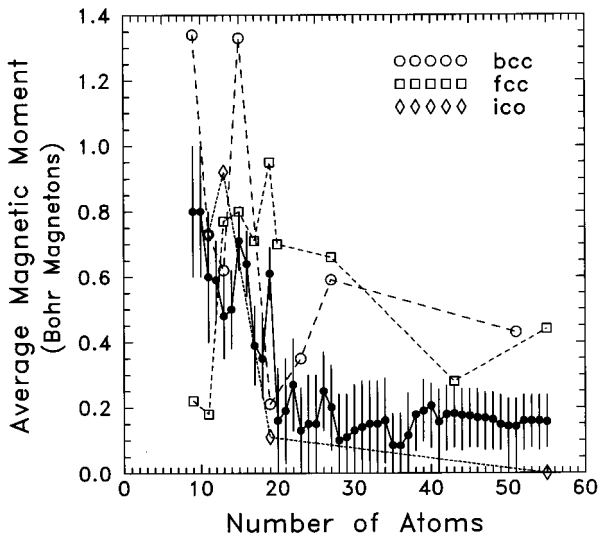


FIG. 3. Average magnetic moment $\bar{\mu}_N$ of Rh_N clusters as a function of N . The open circles correspond to bcc-like clusters, the squares to fcc-like clusters, and the diamonds to icosahedral-like clusters. The experimental results from Ref. 14 are indicated by dots and error bars. The lines are just a guide to the eye.

According to our calculations, the size dependence of $\bar{\mu}_N$ in the range $15 \leq N \leq 20$ indicates that the underlying cluster structure is fcc-like. Two arguments support this statement. First, the largest $E_{\text{coh}}(N)$ is obtained for the fcc clusters ($15 \leq N \leq 20$) and, second, the other considered structures (bcc and icosahedral) fail to reproduce all the observed oscillations¹⁴ (see Fig. 3). The interpretation of the minimum in $\bar{\mu}_N$ at $N=13$ appears to be more subtle. Assuming that small Rh_N clusters have compact structures, it seems reasonable that Rh_{13} should be a highly symmetric cluster with a central atom and the complete shell of its first NN (e.g., fcc, hcp, or icosahedral). In this case, the single-particle spectrum presents many degeneracies which tend to favor a relatively large $\bar{\mu}_{13}$. Moreover, adding or removing an atom from the outer shell would necessarily reduce the cluster symmetry. Thus, a maximum at $N=13$ should be obtained rather than the minimum observed in the experiment. According to our results, the minimum in $\bar{\mu}_N$ at $N=13$ is associated with a structural change. In fact, we obtain that the low-symmetry bcc-like geometry (with an incomplete second NN shell) is more stable than the higher-symmetry fcc or icosahedral structures. The stability of the bcc structure is thus responsible for the drop of $\bar{\mu}_N$ at $N=13$.

In Fig. 3 results are given for $\bar{\mu}_N$ of Rh_N for the different considered structures. A remarkable size and structural dependence is revealed which is characteristic of materials showing weak (unsaturated) itinerant magnetism. Let us recall that the microscopic origin of this behavior is the availability of holes to be polarized (up to two per atom, for $n_d=8.0$) together with the strong sensitivity of the electronic structure around ε_F to the cluster size and geometry. It seems very difficult to derive simple rules or trends concerning the changes in $\bar{\mu}_N$ as a function of cluster size and structure. Nonetheless, the role of cluster symmetry should be underlined. Notice that the structures considered here — a central atom with an increasing number of its first, second, etc., NN — are such that highly symmetric clusters are obtained

when a shell of NN is closed (e.g., at $N=13$ and 19 for icosahedral or fcc clusters or at $N=15$ for bcc clusters). In these cases, larger degeneracies are present in the single-particle spectrum which favor the development of a larger magnetization. Adding or removing an atom from a closed-shell cluster reduces the symmetry. Thus, some degeneracies are removed and often a reduction of $\bar{\mu}_N$ results. This explains qualitatively the maxima in $\bar{\mu}_N$ obtained at $N=13$ (icosahedral), at $N=19$ (icosahedral or fcc-like) and at $N=15$ (bcc-like). However, more complicated energy-level shifts associated with redistributions of the spin density, to bond-length changes, etc., may mask or reduce this simple symmetry effect. Such a situation occurs for fcc Rh_N around $N=13-15$. The importance of bond-length relaxation to the magnetic properties, which of course depends on the cluster structure, should be also emphasized. For instance, the particularly small $\bar{\mu}_N$ obtained for icosahedral Rh_{19} and Rh_{55} and as well as for bcc Rh_{19} are a consequence of significant contractions (see Table I).

Concerning the distribution of the local magnetic moments $\mu(i)$ and the magnetic order within the cluster, we may observe that the bcc clusters order ferromagnetically [i.e., all the $\mu(i)$ have the same sign]. The only exception among the considered cluster sizes is the 11-atom cluster which shows a small antiparallel local moment at the central atom (see Table I). The $\mu(i)$ in bcc Rh clusters tend to increase as we go from the center to the surface of the cluster. As discussed in Ref. 9 this can be qualitatively understood as a consequence of the reduction of the local coordination number and the resulting reduction of the effective local bandwidth. A similar behavior has been observed in bcc Fe clusters.⁹ The compact structures, such as fcc and icosahedral, present a more complex magnetic behavior. In these cases the magnetic order within Rh_N is often antiferromagneticlike, i.e., $\mu(i)$ changes sign for different i (see, for example, the fcc clusters having $N=9, 11, 15, 20$, and 55 or the icosahedral clusters with $N=11$ and 19). A similar behavior has been found in fcc Rh surfaces and thin films³⁴ as well as in fcc Fe clusters.⁹ Moreover, notice that in fcc and icosahedral Rh_N (e.g., for $N=19$) the magnetic moments at the central atom $\mu(1)$ are often larger than at the cluster surface. In other words, although the reduction of coordination number z with respect to the bulk is responsible for the onset of magnetism in Rh_N , the atoms showing the smallest z do not carry the largest magnetic moments. In this context, it is worth remarking that the self-consistent numerical solution of Eqs. (2.3)–(2.5) can be quite delicate in the case of Rh_N . In order to avoid getting trapped in a wrong solution we have considered, for all of the studied clusters, several different distributions of the spin-polarized density as starting points of the iterative self-consistent procedure (in some cases up to 10–15). Furthermore, reliable stable results for the local magnetic moments require high accuracy, i.e., very small differences between the input and output $\langle \hat{n}_{i\alpha\sigma} \rangle$ (typically at least 10^{-5} electrons per atom). This is particularly important when one or more peaks in the DOS are close to the Fermi energy ε_F , for example, when a spin flip occurs (see Ref. 11). In these cases we find density distributions $\langle \hat{n}_{i\alpha\sigma} \rangle$ which seem to be self-consistent within an error of 10^{-2} electrons per atom, but which are unstable if a higher

accuracy is imposed. For instance, in the case of the twisted double-square Rh_9 (tw_9) such an unstable solution may yield $\bar{\mu}_9=0.4\mu_B$ in contrast to the fully converged result $\bar{\mu}_9=0.66\mu_B$. However, if the accuracy is sufficiently high, we have not encountered multiple solutions to Eqs. (2.3)–(2.5), at least for the relevant geometries and bond lengths.

Concerning the sensitivity of our results to the value of the exchange integral J , the most delicate of the model parameters, the following may be observed. For magnetic $3d$ TM's, J is usually set to reproduce the correct value of the bulk magnetization at $T=0$. In the case of elements which are paramagnetic in the bulk, the magnetic properties of low-dimensional systems are often analyzed as a function of J .¹³ In this work we have used $J=0.48$ eV as derived from LSDA calculations on Rh bulk.^{27–29} In order to assess the effect of varying J on the magnetic properties of Rh_N , we have performed calculations for icosahedral clusters with $N=13$ and $N=55$ atoms by setting $J=0.60$ eV. In this case we obtain $\bar{\mu}_{13}=1.08\mu_B$ and $\bar{\mu}_{55}=0.04\mu_B$ which should be compared to the $J=0.48$ eV results, $\bar{\mu}_{13}=0.92\mu_B$ and $\bar{\mu}_{55}=0.0\mu_B$. In contrast to similar calculations on Rh films,³⁴ the average magnetic moments of these Rh clusters are not strongly modified even by rather large changes in J (about 25%). This indicates that reasonable variations of J should not alter the calculated trends in size dependence of $\bar{\mu}_N$, in particular concerning the oscillations.

Finally, we would like to compare our results for $\bar{\mu}_N$ of Rh_N with previous calculations. For bcc-like Rh_9 we find $\bar{\mu}_9(\text{bcc})=1.34\mu_B$, which is considerably larger than the value obtained by Li *et al.* using the LSDA ($\bar{\mu}_9=0.56\mu_B$).¹⁹ According to our calculation, the most stable structure is the twisted double-square pyramid with $\bar{\mu}_9=0.66\mu_B$ which has not been studied yet by *ab initio* methods. For Rh_{13} several independent calculations have been reported. In this case we obtain that the most stable structure is a bcc-like arrangement yielding $\bar{\mu}_{13}=0.62\mu_B$. To our knowledge, this structure has not been considered before. For fcc-like Rh_{13} we find $\bar{\mu}_{13}(\text{fcc})=0.73\mu_B$, whereas Galicia¹⁵ reported $\bar{\mu}_{13}(\text{fcc})=1.00\mu_B$, Reddy *et al.*¹⁶ $\bar{\mu}_{13}(\text{fcc})=1.46\mu_B$, and Jinlong *et al.*¹⁷ $\bar{\mu}_{13}(\text{fcc})=1.46\mu_B$. For the icosahedral configuration, our result is $\bar{\mu}_{13}(\text{ico})=0.92\mu_B$ whereas Reddy *et al.*¹⁶ found $\bar{\mu}_{13}(\text{ico})=1.62\mu_B$, Jinlong *et al.*¹⁸ $\bar{\mu}_{13}(\text{ico})=1.15\mu_B$, and Li *et al.*¹⁹ $\bar{\mu}_{13}(\text{ico})=0.69\mu_B$. It has been argued that the discrepancies in the previous *ab initio* calculations for the icosahedral 13-atom cluster might be related to the presence of multiple solutions to the Kohn-Sham equations.^{18,19} For $N=19$ and 43 we find similarly dispersed results. While our self-consistent tight-binding calculations yield $\bar{\mu}_{19}(\text{fcc})=0.95\mu_B$ and $\bar{\mu}_{43}(\text{fcc})=0.28\mu_B$, LSDA studies yield $\bar{\mu}_{19}(\text{fcc})=0.43\mu_B$ and $\bar{\mu}_{43}(\text{fcc})=0.016\mu_B$ (Ref. 19) or $\bar{\mu}_{19}(\text{fcc})=1.42\mu_B$.¹⁸ In general, our results for $\bar{\mu}_N$ overestimate the experimental results for $N=19$ and 43, whereas those of Li *et al.*¹⁹ underestimate them.

IV. DISCUSSION

The magnetism of small Rh_N clusters has been investigated in the framework of a d -band tight-binding model Hamiltonian including Coulomb interactions in the unrestricted Hartree-Fock approximation. Three main cluster ge-

ometries representative of different local atomic environments (viz., fcc-, bcc-, and icosahedral-like) have been considered. The interatomic NN bond length were optimized by maximizing the cluster cohesive energy including in particular the magnetic contributions due to the environment dependence of the local magnetic moments. The calculated size and structural dependence of the magnetic properties of Rh clusters is remarkably rich and rather complex. Depending on the interatomic bond length and on the cluster structure, we find important variations of spin density within the cluster, leading to both ferromagneticlike and antiferromagneticlike order. This results in oscillations of the average magnetic moment per atom $\bar{\mu}_N$ as a function of N . Simple trends, for example, relating the local magnetic moments to the local environment of the atoms,⁹ seem very difficult to derive. Our results for $\bar{\mu}_N$ are in good qualitative agreement with experiment in particular concerning its oscillations in the size range $9 \leq N \leq 20$. For $N > 20$ our calculations overestimate by about $(0.2-0.3)\mu_B$ the $\bar{\mu}_N$ derived from experiment.¹⁴

In spite of these results, several important aspects of the problem still remain to be addressed. First, it would be interesting to investigate to what extent our results could be modified by certain desirable improvements on the model Hamiltonian. For instance, including the sp valence electrons explicitly in the calculations could affect the relative stability of structures which are close in energy and could thus modify indirectly the magnetic behavior, even if the latter is dominated by the d electrons. In order to investigate this problem we have determined the electronic and magnetic properties of Rh clusters by solving self-consistently a more realistic spd -band model Hamiltonian.^{23,35} The hopping integrals $t_{ij}^{\alpha\beta}$ used in these calculations are obtained by fitting the band structure of Rh solid.³⁰ For simplicity we neglect the differences between s and p Coulomb integrals (i.e., $U_{ss}=U_{sp}=U_{pp}$ and $U_{sd}=U_{pd}$) and take the ratios between the direct Coulomb integrals $U_{ss}:U_{sd}:U_{dd}$ from atomic Hartree-Fock calculations.³⁶ Exchange integrals other than J_{dd} are neglected.^{23,35} As representative examples we consider the fcc, bcc, and icosahedral Rh_{13} clusters. These are particularly interesting in order to verify two main conclusions derived from d -band-only calculations, namely, that the low-symmetry bcc-like Rh_{13} is more stable than the fcc and icosahedral Rh_{13} and that the average magnetic moment per atom corresponding to the bcc structure is particularly small. In relation to experiment, this could explain the minimum in $\bar{\mu}_N$ vs N observed at $N=13$.¹⁴ While the spd calculations — summarized in Table II — confirm in fact the conclusions inferred in the framework of the simpler d -band model, comparison between Tables I and II also reveals interesting differences which allow us to quantify sp -electron effects. First of all, we observe that the sp -electron contribution to the cohesive energy is very important ($E_{\text{coh}}^{spd}-E_{\text{coh}}^d \approx 3.2$ eV/atom). However, in spite of this, sp binding does not modify significantly either the bond-length contraction R/R_0 or the relative stability between the different considered structures. This is consistent with the belief that d -electron states should play the dominant role on the structural stability of TM clusters, since the distance and angular dependence of d -electron interactions

TABLE II. Electronic and magnetic properties of Rh_{13} clusters as obtained by including s , p , and d electrons self-consistently in the calculations. As in Table I, results are given for the cohesive energy per atom, E_{coh} (in eV), the equilibrium bond length R/R_0 (R_0 = bulk NN distance), the average magnetic moment per atom $\bar{\mu}_N$ (in units of μ_B), and the local magnetic moments $\mu(i)$ at the different symmetry atoms i (see Fig. 1).

Cluster	E_{coh}	R/R_0	$\bar{\mu}_N$	$\mu(1)$	$\mu(2)$	$\mu(3)$
bcc ₁₃	5.68	0.94	0.38	-0.05	0.37	0.51
ico ₁₃	5.61	0.93	1.15	1.42	1.13	
fcc ₁₃	5.64	0.97	1.00	1.39	0.97	

are much stronger than for sp electrons.^{9,37} Concerning the magnetic behavior, we obtain that bcc-like Rh_{13} shows a particularly small average magnetic moment per atom $\bar{\mu}_{13}^{sp,d} = 0.38\mu_B$, which is consistent with the experimental result [$\bar{\mu}_{13}^{\text{expt}} = (0.48 \pm 0.13)\mu_B$ (Ref. 14)] and with the presence of a minimum in $\bar{\mu}_N$ at $N = 13$. In contrast, for fcc and icosahedral Rh_{13} , $\bar{\mu}_{13}^{sp,d} \approx 1\mu_B$. These trends are in agreement with the d -band-only results ($|\mu_{13}^{sp,d} - \mu_{13}^d| \approx 0.2\mu_B$; see Tables I and II). The local magnetic moments are in general more sensitive to the details of the electronic structure and thus to sp - d hybridization effects. This is particularly noticeable in the magnetic moment at the central atom $\mu(1)$ (compare Table I for $N = 13$ and Table II). In the case of fcc and icosahedral Rh_{13} , $\mu(i)$ and $\bar{\mu}_{13}$ are enhanced when sp electrons are taken into account. This is in a sense remarkable since in first approximation the sp - d hybridizations should increase the broadening of the d states and thus tend to reduce the local magnetic moments. For the considered clusters we do not find significant sp - d charge transfer [$n_d(i) \approx 7.8$ – 8.0].

For small clusters (e.g., fcc-like with $N = 13$, bcc-like with $N = 9$, etc.) we expect that the bond-length relaxation should be the same or nearly the same for all bonds. However, for larger clusters, different relaxations should be allowed for inner and outer atoms. In order to quantify the importance of nonuniform relaxation on the magnetic behavior, we have performed calculations on the fcc-like Rh_{19} , allowing different relaxations on atoms having different local environments. We obtain that the distance between the central atom and its first NN shell is $R/R_0 = 0.975$, while the distance between the atoms in the first and second NN shell is $R/R_0 = 0.955$. If only uniform relaxation is allowed, we have $R/R_0 = 0.97$. The interatomic distance at the surface and in the interior of Rh_{19} differ by about 2%. As physically expected, nonuni-

form relaxation yields a larger contraction at the cluster surface. This improved geometry optimization does not modify the relative stability between fcc, bcc, and icosahedral structures, since E_{coh} is increased by only 0.01 eV.³⁸ Concerning the magnetic properties, we obtain the same value for the average magnetic moment per atom and only small changes in the local magnetic moments: for the nonuniformly relaxed Rh_{19} , $\mu(1) = 1.3\mu_B$, $\mu(2) = 1.05\mu_B$, and $\mu(3) = 0.62\mu_B$. Therefore, performing these more demanding calculations should not modify our conclusions on the magnetic behavior of small Rh_N for the considered types of cluster geometries. Nevertheless, an improved accuracy of the electronic structure, the cohesive energy, and the interatomic forces, together with the application of fully relaxed geometry optimization methods (molecular dynamics or Monte Carlo), would be certainly worthwhile. Taking into account the results discussed in the previous section, a remarkable interplay between magnetism and structure may be expected in Rh_N , which should reveal very interesting, though quite complex, potential energy surfaces. At the same time, the possibility of noncollinear spin arrangements should be investigated. This may lead to substantial improvements in the ground-state energy, if antiferromagnetic frustrations are present in compact structures.³⁹ However, notice that many of the Rh clusters studied in this paper show ferromagneticlike order and that in such cases noncollinear spin arrangements are very unlikely. Last, but not least, remains the role of electronic correlations, which are expected to affect the stability of magnetism in general and the onset of magnetism in $4d$ TM clusters in particular.²¹ Besides the fundamental interest of this question, small Rh_N clusters are an excellent system to investigate the problem of correlations in finite systems, since the observed size dependence of $\bar{\mu}_N$ is far from trivial.

We would like to conclude by emphasizing the importance of the interplay between geometrical structure and itinerant magnetism in small clusters. Our model calculations have allowed us to study several low-symmetry structures and revealed that they are crucial for the size dependence of the magnetic properties.

ACKNOWLEDGMENTS

This work was supported in part by CONACyT (Mexico) and by a CONACyT-CNRS grant. The Institut de Physique et Chimie des Matériaux de Strasbourg and the Laboratoire de Physique Quantique (Toulouse) are Unités Mixtes de Recherche associated with the CNRS. The computer resources provided by CENCAR (University of Guadalajara, Mexico) are gratefully acknowledged.

¹F. Hund, *Linienpektren und periodisches System der Elemente* (Springer, Berlin, 1927), p. 124; E. U. Condon and G. H. Shortley, *The Theory of Atomic Spectra* (Cambridge University Press, Cambridge, England, 1957), p. 209.

²C. Kittel, *Introduction to Solid State Physics* (John Wiley and Sons, Inc., New York, 1976).

³Proceedings of the Seventh International Symposium on Small Particles and Inorganic Clusters (ISSPIC7), Kobe, Japan, 1994 [Surf. Rev. Lett. **3** (1996)].

⁴C. Y. Yang, K. H. Johnson, D. R. Salahub, J. Kaspar, and R. P. Messmer, Phys. Rev. B **24**, 5673 (1981); D. R. Salahub and R. P. Messmer, Surf. Sci. **106**, 415 (1981).

⁵K. Lee, J. Callaway, and S. Dhar, Phys. Rev. B **30**, 1724 (1985); K. Lee, J. Callaway, K. Wong, R. Tang, and A. Ziegler, *ibid.* **31**, 1796 (1985).

⁶D. M. Cox, D. J. Trevor, R. L. Whetten, E. A. Rohfing, and A. Kaldor, Phys. Rev. B **32**, 7290 (1985).

⁷I. M. L. Billas, J. A. Becker, A. Châtelain, and W. A. de Heer,

- Phys. Rev. Lett. **71**, 4067 (1993); I. M. L. Billas, A. Châtelain, and W. A. de Heer, *Science* **265**, 1662 (1994).
- ⁸J. P. Bucher, D. C. Douglass, and L. A. Bloomfield, *Phys. Rev. Lett.* **66**, 3052 (1991); *Phys. Rev. B* **45**, 6341 (1992); D. C. Douglass, A. J. Cox, J. P. Bucher, and L. A. Bloomfield, *ibid.* **47**, 12 874 (1993).
- ⁹G. M. Pastor, J. Dorantes-Dávila, and K. H. Bennemann, *Physica B* **149**, 22 (1988); *Phys. Rev. B* **40**, 7642 (1989).
- ¹⁰F. Liu, S. N. Khanna, and P. Jena, *Phys. Rev. B* **43**, 8179 (1991).
- ¹¹J. Dorantes-Dávila, H. Dreyssé, and G. M. Pastor, *Phys. Rev. B* **46**, 10 432 (1992).
- ¹²K. Lee and J. Callaway, *Phys. Rev. B* **48**, 15 358 (1993).
- ¹³J. Dorantes-Dávila and H. Dreyssé, *Phys. Rev. B* **47**, 3857 (1993); P. Alvarado, J. Dorantes-Dávila, and H. Dreyssé, *ibid.* **50**, 1039 (1994).
- ¹⁴A. J. Cox, J. G. Louderback, and L. A. Bloomfield, *Phys. Rev. Lett.* **71**, 923 (1993); A. J. Cox, J. G. Louderback, S. E. Apsel, and L. A. Bloomfield, *Phys. Rev. B* **49**, 12 295 (1994).
- ¹⁵R. Galicia, *Rev. Mex. Fis.* **32**, 51 (1985).
- ¹⁶B. V. Reddy, S. N. Khanna, and B. I. Dunlap, *Phys. Rev. Lett.* **70**, 3323 (1993).
- ¹⁷Y. Jinlong, F. Toigo, W. Kelin, and Z. Manhong, *Phys. Rev. B* **50**, 7173 (1994).
- ¹⁸Y. Jinlong, F. Toigo, and W. Kelin, *Phys. Rev. B* **50**, 7915 (1994).
- ¹⁹Z.-Q. Li, J.-Z. Yu, K. Ohno, and Y. Kawazoe, *J. Phys. Condens. Matter* **7**, 47 (1995).
- ²⁰B. Piveteau, M.-C. Desjonquères, A. M. Olés, and D. Spanjaard, *Phys. Rev. B* **53**, 9251 (1996).
- ²¹G. M. Pastor, R. Hirsch, and B. Mühlischlegel, *Phys. Rev. Lett.* **72**, 3879 (1994); *Phys. Rev. B* **53**, 10 382 (1996).
- ²²R. H. Victora and L. M. Falicov, *Phys. Rev. Lett.* **55**, 1140 (1985).
- ²³A. Vega, J. Dorantes-Dávila, L. C. Balbás, and G. M. Pastor, *Phys. Rev. B* **47**, 4742 (1993).
- ²⁴R. Haydock, in *Solid State Physics*, edited by H. Ehrenreich, F. Seitz, and D. Turnbull (Academic, New York, 1980), Vol. 35, p. 215.
- ²⁵J. P. Bucher and L. A. Bloomfield, *Int. J. Mod. Phys. B* **7**, 1079 (1993).
- ²⁶V. Heine, *Phys. Rev.* **153**, 673 (1967).
- ²⁷N. E. Christensen, O. Gunnarsson, O. Jepsen, and O. K. Andersen, *J. Phys. (Paris) Colloq.* **49**, C8-17 (1988); O. K. Andersen, O. Jepsen, and D. Glötzel, in *Highlights of Condensed Matter Theory*, edited by F. Bassani, F. Fumi, and M. P. Tosi (North-Holland, Amsterdam, 1985), p. 59.
- ²⁸In Ref. 27 the spin splitting induced in bulk Rh by a small external magnetic field h ($h \rightarrow 0$) is calculated by means of an integration of the exchange-correlation potential involving the LMTO wave functions $\psi(\vec{k})$. The resulting $J(\vec{k})$ is then averaged over the paramagnetic Fermi surface (see Ref. 27 for further details).
- ²⁹G. Stollhoff, A. M. Oles, and V. Heine, *Phys. Rev. B* **41**, 7028 (1990).
- ³⁰D. A. Papaconstantopoulos, *Handbook of the Band Structure of Elemental Solids* (Plenum, New York, 1986).
- ³¹See, for instance, M. C. Desjonquères and D. Spanjaard, *Concepts in Surface Physics* (Springer-Verlag, Berlin, 1996).
- ³²W. A. Harrison, *Electronic Structure and the Properties of Solids* (Freeman, San Francisco, 1980); M. van Schilfhaarde and W. A. Harrison, *Phys. Rev. B* **33**, 2653 (1986).
- ³³J. Dorantes-Dávila, A. Vega, and G. M. Pastor, *Phys. Rev. B* **47**, 12 995 (1993); J. Dorantes-Dávila and G. M. Pastor, *ibid.* **51**, 16 627 (1995).
- ³⁴A. Chouairi, H. Dreyssé, H. Nait-Laziz, and C. Demangeat, *Phys. Rev. B* **48**, 7735 (1993); A. Mokrani and H. Dreyssé, *Solid State Commun.* **90**, 31 (1994).
- ³⁵A. Vega, L. C. Balbás, J. Dorantes-Dávila, and G. M. Pastor, *Phys. Rev. B* **50**, 3899 (1994).
- ³⁶J. B. Mann (unpublished).
- ³⁷G. M. Pastor, J. Dorantes-Dávila, and K. H. Bennemann, *Chem. Phys. Lett.* **148**, 459 (1988).
- ³⁸A. Vega *et al.*, *Phys. Rev. B* **48**, 985 (1993); A. Vega, L. C. Balbás, and H. Dreyssé, *J. Magn. Magn. Mater.* **121**, 177 (1993).
- ³⁹M. A. Ojeda-López, J. Dorantes-Dávila, and G. M. Pastor (unpublished).